System implementation requires adding a magnetometer, a control amplifier, and the electromagnet to the attitude control system. A single gimbaled magnet or three fixed magnets, of air-coil or iron-core construction, may be used. In all cases, the total weight of conductor and power supply (solar array, batteries, and control amplifier) is a minimum if the conductor weight equals the power supply weight.

Although the total weight of magnet plus power supply is smaller for a gimbaled design, the additional weight and complexity of the gimbal mechanism and the space required to accommodate the moving magnet make the three-magnet design, in particular the air coils, more attractive.

Placing an upper bound on $|\mathbf{M}|$, the magnitude of the magnetic moment, allows an iron-core weight savings of 15%, but results in little weight savings for air-coil designs. Day-only dumping with a constant $|\mathbf{M}|$ eliminates the need for battery capacity, but a larger magnet size is required because of the reduced dumping time.

References

[1] White, J. S., Shigemoto, F. H., and Bourguin, K., "Satellite Attitude Control Utilizing the Earth's Magnetic Field," TN D-1068, Aug. 1961, NASA.

[2] Brown, S. C., "An Analytical Comparison of Some Electromagnetic Systems for Removing Momentum Stored by a Satellite Attitude Control System," TN D-2693, March 1965, NASA.

[3] Wheeler, P. C., "Magnetic Attitude Control of Rigid, Axially Symmetric, Spinning Satellites in Circular Earth Orbits," CR-313, Oct. 1965, NASA.

[4] Abbott, J. K., "Momentum Unloading Systems—Design of Magnetic Unloading Actuators," N67-36678, Jan. 1967, Royal Aircraft Establishment, Farnborough, England.

[5] Buckingham, A. G., "A Method of Attitude Control Utilizing the Earth's Magnetic Field for Space Vehicles," Rept. AA-2333, 1961, Westinghouse Electric Corp., Air Arm Division, Baltimore, Md.

[6] Hart, L. R. et al., "Application of Magnetic Torquing for Desaturation of Control Moment Gyros in Space Vehicle Control," TR AFFDL-TR-67-8, June 1967, Westinghouse Defense and Space Center, Baltimore, Md.

[7] Olsen, R., "OAO Magnetic Unloading System Performance in the Presence of a Realistic Earth Field," Rept. SYST-252R-7.0, May 1968, Grumman Aircraft Engineering Corp., Bethpage, N.Y.

[8] Blakemore, D. J., "Magnetic Torquing Scheme," *AIAA Journal*, Vol. 1, No. 8, Aug. 1963, pp. 1888–1889.

[9] Adams, J. J. and Brissenden, R. F., "Satellite Attitude Control Using a Combination of Inertia Wheels and a Bar Magnet," TN D-626, Nov. 1960, NASA.

[10] Levidow, W., "Use of Magnetic Torque for CMG Momentum Management," TM 69-1022-8, Dec. 1969, Bellcomm, Inc., Washington, D.C.

OCTOBER 1970 J. SPACECRAFT VOL. 7, NO. 10

Design of an Optimal-Adaptive Digital Autopilot

N. N. PURI*

Rutgers University, New Brunswick, N.J.

The heart of this autopilot design for the flight path control of an aerospace vehicle is a digital computer with three software subroutines for identification, optimal synthesis, and digital compensation. Vehicle motion is described by linear differential equations whose parameters change over a very wide range during the flight and are unknown except for some a priori guess. An identification algorithm based upon discrete orthogonal functions is used to identify the flight motion parameters. An optimization algorithm based upon quadratic performance index determines the closed-loop characteristic polynomial, which when combine with identified flight motion parameters yields the suitable compensation.

Nomenclature

$A_k^{(j)}$	= Fourier coefficients of $x_j(n)$ with respect to orthogonal set $\varphi_k(n)$
$a_n^{(j)},b_k^{(j)}$	= coefficients of z^{-n} in the series expansion of the numerator and denominator, respectively, of $G^{(j)}(z), n = 0,1,2,\ldots$
$B_k^{(j)}$	= Fourier coefficients of $u_j(n)$
β	= performance index parameter
c_k	= coefficients of z^k and z^{-k} in $F(z)$
$D(s),D(z)$	= autopilot transfer function
$G^{(j)}(z),D^{(j)}(z)$	= vehicle and autopilot transfer functions computed from $\{x_j(n)\}_0^{2N}$ and $\{u_j(n)\}_0^{2N}$
$F(z)$	= optimization polynomial
$G(s),G(z)$	= vehicle transfer function
I	= performance index
$2N$	= number of samples required for vehicle dynamic identification
T	= identification time
$u(t)$	= vehicle input or control signal, measured
$u^*(t)$	= vehicle input, without noise
$x(t),x^*(t)$	= vehicle output, measured and without noise
$x_j(n),u_j(n)$	= sampled values of $x(t)$ and $u(t)$ at $t = (j + n)T/2N \quad j = 0, \ldots, \infty, n = 0, \ldots, 2N$
$v(t),\omega(t)$	= input, output noise
$\{\varphi_k(n)\}_0^\infty$	= set of orthogonal functions, $n = 0, \ldots, \infty$
$\Phi_k(z)$	= Z transform of $\varphi_k(n)$
s	= Laplace transform variable
z	= Z transform variable = e^{-sT}
$\nabla(z)$	= characteristic polynomial of closed-loop transfer function

Introduction

INTEREST in digital autopilot design has increased in recent years due to rapid advances in digital technology. A conventional autopilot is an analog device that provides some fixed compensation based upon assumed vehicle dynamics and environment. The necessity of providing guidance and navigation functions for aerospace vehicles makes it very attractive to combine all of these functions in a control digital computer. Since the autopilot function in a digital

Received November 11, 1969; revision received May 8, 1970.

* Professor of Electrical Engineering, Department of Electrical Engineering.

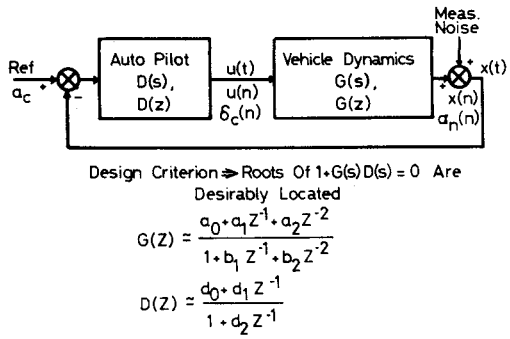

Fig. 1 Conventional autopilot.

device means only a software routine, it can be changed at will without the constraints of a hardwired device. References 1–4 and 7 have shown the feasibility of applying the adaptive control system technology to flight control problems where the environmental parameters such as dynamic pressure vary in 100 to 1 ratio.

In this paper we discuss identification and an optimal compensation algorithm which is quite easy to implement. It works on the incremental basis. Furthermore, after every sample (with the exception of the first few samples after the start), updated identification and compensation parameters are obtained.

Comparison of Autopilots

Figure 1 shows the schematic diagram for a conventional autopilot in which $G(s)$ [or $G(z)$; see Appendix A] represent the vehicle dynamics whose parameters are assumed known and invariant. The autopilot transfer function $D(s)$ [or $D(z)$] takes the form of a lead-lag network. Its coefficients are so chosen that roots of the closed-loop characteristic polynomial $I + G(s)D(s)$ have the desired locations. This can be accomplished by root-locus, Bode or Nyquist plots. The root location sought is such that adequate margin of stability is available under small but adverse variation of parameters of $G(s)$. In case the parameter variations of $G(s)$ are such that a fixed configuration autopilot cannot yield adequate stability margin, a semiadaptive autopilot scheme is needed.

Figure 2 shows the block diagram for the semiadaptive autopilot. The flight path profile is divided into N stages and during each stage the vehicle dynamics are represented by a precomputed transfer function $G^{(j)}(s)(s = 1,2,\ldots,N)$ characterized by the average value of the vehicle parameters. A preprogrammer such as a clock switches in the appropriate autopilot compensation $D^{(j)}(s)(s = 1,\ldots,N)$ such that the desired closed loop roots of $1 + G^{(j)}(s)D^{(j)}(s)$ are obtained.

If the parameter variations of the vehicle dynamics during flight are such that neither of the foregoing method yields adequate stability, the digital autopilot shown in Fig. 3 may do so. Its heart is the computer with three software subroutines: Identification Subroutine I, Optimal Synthesis Subroutine S, and Digital Compensation Subroutine C.

The quantities $u(t)$ and $x(t)$ represent the vehicle input (control signal such as the flap position) and the vehicle output (normal acceleration measured by the accelerometer) respectively, both being contaminated with noises $v(t)$ and $\omega(t)$ due to measurement and turbulence. Thus, $u(t) = u^*(t) + v(t)$, and $x(t) = x^*(t) + \omega(t)$, where the asterisk represents the uncontaminated signals.

The autopilot operation is sequential and is executed as follows: both input and output are sampled to yield $x_j(n)$ and $u_j(n)(n = 0,1,\ldots,2N)$. The quantities

$$\{x_j(n)\}_0^{2N},\ \{u_j(n)\}_0^{2N}$$

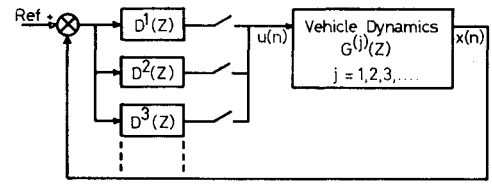

Fig. 2 Semi-adaptive autopilot.

are fed into the identifying routine I to yield the updated transfer function $G^{(j)}(z)$. Thus after the first $2N$ samples, the updated transfer function $G^{(j)}(z)$ is available every $T/2N$ sec. Parameters corresponding to $G^{(j)}(z)$ are supplied to the optimal synthesis subroutine that computes the optimal compensation $D^{(j)}(z)$ and hence $u_j(2N + 1)$.

But

$$u_j(2N + 1) = u_{j+1}(2N)$$
$$u_j(n) = u_{j+1}(n - 1),\ n = 1,2,\ldots,2N \quad (1)$$

Similarly

$$x_j(n) = x_{j+1}(n - 1),\ n = 1,\ldots,2N + 1 \quad (2)$$

Hence a new input and output sampled set

$$\{u_{j+1}(n)\}_0^{2N},\ \{x_{j+1}(n)\}_0^{2N}$$

is available to restart the autopilot.

This method provides continual identification and adaptive compensation. In what follows we shall discuss the algorithms for identification, optimal synthesis and adaptive compensation.

Identification Subroutine

Many methods have been proposed in the literature for the identification of the parameters of the unknown plant. Most methods consist of applying some perturbation signal to the system and recording the response. This approach results in interrupting the normal operation to some extent. Even then the presence of noise makes the identification difficult, if not impossible. Two methods which seem to be of practical value in the present situation are 1) processing of the autocorrelation function of the input and cross-correlation function of the input-output[6] and 2) the least-squares approximation method.[4,11] These methods are explained in Appendix B.

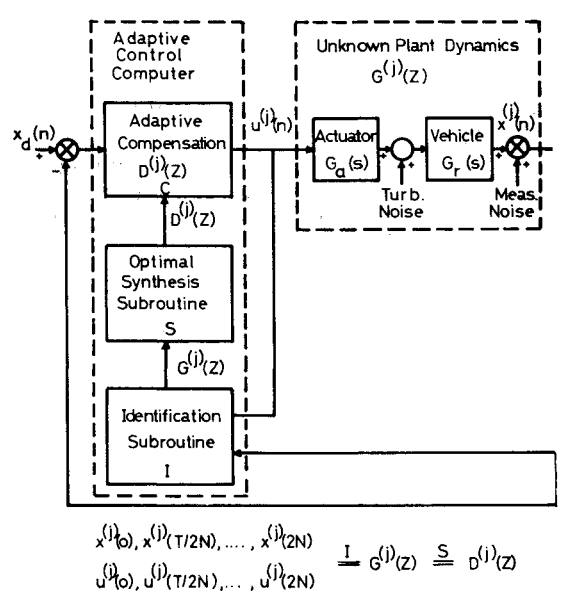

Fig. 3 Continuous adaptive, optimal digital autopilot.

Because of the on-line identification requirement we propose a new and (storage-wise) economical method of identification based upon discrete orthogonal functions. It is described as follows:

$$G^{(j)}(z) = x_j^*(z)/u_j^*(z) \simeq \sum_{n=0}^{2N} x_j^*(n)z^{-n} \Big/ \sum_{n=0}^{2N} u_j^*(n)z^{-n} \quad (3)$$

wherein the infinite upper limit of n ($n = \infty$) is approximated by $2N$, under the assumption that for the frequency domain of interest the contribution from terms higher than z^{-2N} is negligible. Let

$$x_j^*(n) = \sum_{k=1}^{N} A_k^{(j)}\varphi_k(n),\ x_j(n) = x_j^*(n) + \omega_j(n) \quad (4)$$

$$u_j^*(n) = \sum_{k=1}^{N} B_k^{(j)}\varphi_k(n),\ u_j(n) = u_j^*(n) + v_j(n) \quad (5)$$

where $\varphi_k(n)$ are orthogonal functions assumed to be satisfying the following conditions:

$$\sum_{n=0}^{\infty} \varphi_k(n)\varphi_l(n) = \delta_{kl}, \text{ the Kronecker delta} \quad (6)$$

$$\sum_{n=0}^{\infty} \varphi_k(n)\omega_j(n) = \sum_{n=0}^{\infty} \varphi_k(n)v_j(n) = 0 \quad (7)$$

The coefficients $A_k^{(j)}$, $B_k^{(j)}$, again approximating the infinite upper limit by $2N$, are given as:

$$A_k^{(j)} \simeq \sum_{0}^{2N} x_j(n)\varphi_k(n), \qquad B_k^{(j)} \simeq \sum_{0}^{2N} u_j(n)\varphi_k(n) \quad (8)$$

From Eqs. (3–5),

$$G^{(j)}(z) = \sum_{k=1}^{N} A_k^{(j)}\Phi_k(z) \Big/ \sum_{k=1}^{N} B_k^{(j)}\Phi_k(z) \quad (9)$$

where

$$\Phi_k(z) = \sum_{n=0}^{\infty} \varphi_k(n)z^{-n} \qquad k = 1, \ldots, N \quad (10)$$

From Eqs. (8) and (10)

$$G^{(j)}(z) = \sum_{n=0}^{\infty} a_n^{(j)}z^{-n} \Big/ \sum_{n=0}^{\infty} b_n^{(j)}z^{-n} \quad (11)$$

where

$$a_n^{(j)} = \sum_{k=0}^{N} A_k^{(j)}\Phi_k(n) = x_j^*(n) \quad (12)$$

$$b_n^{(j)} = \sum_{k=0}^{N} B_k^{(j)}\Phi_k(n) = u_j^*(n) \quad (13)$$

The quantities that $a_n^{(j)}$ and $b_n^{(j)}$ represent are numerator and denominator coefficients and are called the parameters. In general, $a_n^{(j)}$ and $b_n^{(j)}$ are very small for large values of n. For the application under consideration truncation at $n = 2$ is sufficient. Parameters for higher values of n should be negligible. Thus, the identification scheme comprises Eqs. (8) and (10), and Eqs. (11–13) with $n = 0, 1, 2$. Figure 4 shows the block diagram for the identification subroutine.

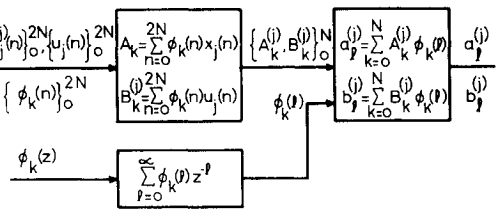

Fig. 4 Identification subroutine.

Choice of Orthogonal Functions $\varphi_k(n)$

Consider the integral, $\oint_{|z|=1} f(z)dz$. If $f(z)$ has all its poles inside (or outside) the unit circle and the difference between the degree of numerator and denominator is at least 2, then

$$\oint_{|z|=1} f(z)dz = 0 \quad (14)$$

Equation (14) forms the basis for construction of different kinds of orthogonal functions. From Parseval's theorem[5]

$$\sum_{n=0}^{\infty} \varphi_k(n)\varphi_l(n) = \frac{1}{2\pi j} \oint_{|z|=1} \Phi_k(z)\Phi_l(z^{-1}) \frac{dz}{z} \quad (15)$$

Hence if $\Phi_k(z)\Phi_l(z^{-1})1/z$ have the same properties as $f(z)$ discussed previously, then $\varphi_k(n)$ and $\varphi_l(n)$ are orthogonal. As an example let us choose the following orthogonal set:

$$\Phi_1(z) = 3^{1/2}/(2z - 1)$$

$$\Phi_2(z) = [(z - 2)/(2z - 1)][8^{1/2}/(3z - 1)]$$

$$\vdots$$

$$\Phi_k(z) = \prod_{m=0}^{k-1} (z - m)[(k + 1)^2 - 1]^{1/2} \Big/ \prod_{m=0}^{k-1} (mz - 1)(k + 1 - z) \quad k = 1, \ldots, \infty \quad (16)$$

It can be easily verified that

$$(1/2\pi j) \oint_{|z|=1} \Phi_k(z)\Phi_l(z^{-1})dz/z = \delta_{kl} \quad (17)$$

Another general set can be written as

$$\Phi_k(z) = \prod_{m=0}^{k-1} F(\alpha_m,z)\Phi(\alpha_k,z) \qquad k = 1, \ldots, \infty \quad (18)$$

where

$$F(\alpha_m,z) = (z - \alpha_m)/(\alpha_m z - 1) \qquad m = 1, \ldots, \infty \quad (19)$$

$$\Phi(\alpha_k,z) = (\alpha_k^2 - 1)^{1/2}/(\alpha_k z - 1),\ |\alpha_k| \geq | \quad (20)$$

Optimal Synthesis Subroutine

In this section we assume that the vehicle transfer function $G^{(j)}(z)$ is known, and at time $t = T + j(T/2N)$ it is described by Eq. (11) with only three terms each in the numerator and denominator. We are interested in computing the closed-loop transfer function so that some performance index I is optimized. For simplicity we shall omit the subscript and superscript j and assume its implicit presence. Thus $x_j(n) = x(n)$, $a_k^{(j)} = a_k$, and $G^{(j)}(z) = G(z)$. We assume that

$$b_0x(n) + b_1x(n - 1) + b_2(n - 2) = a_0u(n) + a_1u(n - 1) + a_2(n - 2) = v(n) \quad (21)$$

Let us choose a performance index[8–10]

$$I = \sum_{n=0}^{\infty} x^2(n) + \beta v^2(n) \equiv \sum_{n=0}^{\infty} F(n) \quad (22)$$

where β is some known constant, and $v(n)$ is given by Eq. (21). Let the optimal output function be given by $x\dagger(n)$. Then the nonoptimal function $x(n)$ can be written as

$$x(n) = x\dagger(n) + \epsilon\eta(n)$$

$$\vdots$$

$$x(n - m) = x\dagger(n - m) + \epsilon\eta(n - m) \quad (23)$$

where $\eta(n)$ is some variation function. The necessary

optimization condition is

$$\partial I/\partial \epsilon|_{\epsilon=0} = 0 \tag{24}$$

From Eqs. (22–24),

$$\frac{\partial I}{\partial \epsilon}\bigg|_{\epsilon=0} = \sum_{n=0}^{\infty}\left[\sum_{k=0}^{2}\frac{\partial F(n+k)}{\partial x(n)}\right]_{\substack{\eta(n)=0\\ x(n)=x\dagger(n)}} \tag{25}$$

Since $\eta(n)$ is an arbitrary function, the optimal synthesis is achieved by

$$\sum_{k=0}^{2}\frac{\partial F(n+k)}{\partial x(n)} = 0 \tag{26}$$

For a general system with order m, the upper index of summation is m. From Eqs. (22) and (26), we obtain

$$c_2x\dagger(n+2) + c_1x\dagger(n+1) + c_0x\dagger(n) + c_1x\dagger(n-1) + c_2x\dagger(n-2) = 0 \tag{27}$$

where

$$c_2 = \beta b_0b_2,\ c_1 = \beta(b_0b_1 + b_1b_2),\ c_0 = \beta(b_0^2 + b_1^2 + b_2^2) + 1 \tag{28}$$

Equation (27) represents the discrete Euler-Lagrange equation whose coefficients c_m depend upon the value of β and the vehicle dynamics coefficients $b_m (m = 0, 1, 2)$. The characteristic equation corresponding to Eq. (8) is

$$F(z) = \sum_{k=0}^{2} c_kz^k + \sum_{k=1}^{2} c_kz^{-k} \tag{29}$$

For the identified transfer function at $t = T + jT/2N$ having an order m, the coefficients c_k and the polynomial $F(z)$ are designated by superscript "j." Equation (29) is such that if z is replaced with z^{-1}, it remains unchanged. Thus, for every root $(z + \alpha)$ there is a root $(\alpha z + 1)$; i.e., for every root outside the unit circle, there is a corresponding root inside the unit circle. Since the roots outside the unit circle represent an unstable response, the closed-loop compensation must be so chosen that the residue corresponding to the unstable roots is zero. This suggests that if we can write

$$F(z) = k\nabla(z)\nabla(z^{-1}) \tag{30}$$

then $\nabla(z)$, with roots inside the unit circle in the z plane can be chosen to represent the characteristic polynomial for the closed loop system. Thus from Eqs. (29) and (30)

$$\nabla(z) = z^2 + \alpha_1z + \alpha_0 \tag{31}$$

where

$$\alpha_1 + \alpha_1/\alpha_0 = c_1/c_2,\ 1 + \alpha_0^2 + \alpha_1^2/\alpha_0 = c_0/c_2 \tag{32}$$

In general, higher-order systems [Eq. (32)] are nonlinear and tedious to solve. Since the coefficients c_m do not change very much from $t = (1 + j - 1/2N)T$ to $t = (1 + j/2N)T$, it is appropriate for computational economy to linearize Eq. (32). Thus, if Eq. (32) can be written as the vector equation

$$\mathbf{f}[\boldsymbol{\alpha}^{(j)}] = \mathbf{g}[\mathbf{c}^{(j)}] = \mathbf{g}^{(j)} \tag{33}$$

then, let

$$\boldsymbol{\alpha}^{j} = \boldsymbol{\alpha}^{(j-1)} + \delta\boldsymbol{\alpha}^{(j)} \tag{34}$$

Linearizing Eq. (33) yields

$$\delta\boldsymbol{\alpha}^{(j)} = (\nabla_{\alpha}\mathbf{f}^T)^{-1}(\mathbf{g}^{(j)} - \mathbf{f}^{(j-1)}) \tag{35}$$

where $(\nabla_{\alpha}f^T)$ represents the Jacobian and $\mathbf{f}^{(j-1)}$ is $\mathbf{f}(\boldsymbol{\alpha})$ both evaluated for $\alpha = \boldsymbol{\alpha}^{(j-1)}$. The quantity $\boldsymbol{\alpha}$ is a $(m - 1)$ vector whose components are α_0, α_1, etc. Thus, $\alpha_0^{(j)}$, $\alpha_1^{(j)}$, etc. are computed from Eq. (35), starting with some precomputed initial values $\alpha_0^{(0)}$, $\alpha_1^{(0)}$, etc. A final check should be made to insure that the roots of the polynomial $\nabla^{(j)}(z)$ lie within the unit circle.

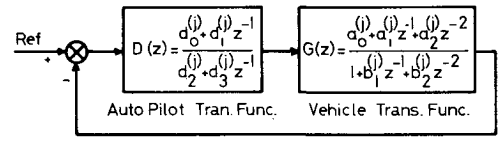

Fig. 5 Instantaneous closed-loop transfer function.

Adaptive and Optimal Compensation

From Fig. 5 the optimal adaptive closed-loop transfer function $K^{(j)}(z)$ is given by

$$K^{(j)}(z) = G^{(j)}(z)D^{(j)}(z)/[1 + G^{(j)}(z)D^{(j)}(z)] \tag{36}$$

Let us assume the compensation $D^{(j)}(z)$ of the form shown in Fig. 5, and $G^j(z)$ as given by Eq. (11) truncated at $n = 2$. From these, the closed-loop characteristic polynomial $\Delta^{(j)}(z)$ is given as

$$\nabla^{(j)}(z^{-1}) = [b_0^{(j)} + b_1^{(j)}z^{-1} + b_2^{(j)}z^{-2}][d_2^{(j)} + d_3^{(j)}z^{-1}] + [a_0^{(j)} + a_1^{(j)}z^{-1} + a_2^{(j)}z^{-2}][d_0^{(j)} + d_1^{(j)}z^{-1}] \tag{37}$$

From Eq. (30) the optimal adaptive closed-loop characteristic polynomial is computed as

$$\nabla^{(j)}(z^{-1}) = z^{-2} + \alpha_1^{(j)}z^{-1} + \alpha_0^{(j)} \tag{38}$$

From Eqs. (37) and (38)

$$\mathbf{d}^{(j)} = [\mathbf{p}^{(j)}]^{-1}\boldsymbol{\alpha}^{(j)} \tag{39}$$

where

$$\mathbf{d}^{(j)} = \begin{bmatrix} d_0^{(j)} \\ d_1^{(j)} \\ d_2^{(j)} \\ d_3^{(j)} \end{bmatrix},\ \boldsymbol{\alpha}^{(j)} = \begin{bmatrix} \alpha_0^{(j)} \\ \alpha_1^{(j)} \\ 1 \\ 0 \end{bmatrix} \tag{40}$$

$$\mathbf{p}^{(j)} = \begin{bmatrix} 0 & a_2^{(j)} & 0 & b_2^{(j)} \\ a_2^{(j)} & a_1^{(j)} & b_2^{(j)} & b_1^{(j)} \\ a_1^{(j)} & a_0^{(j)} & b_1^{(j)} & b_0^{(j)} \\ a_0^{(j)} & 0 & b_0^{(j)} & 0 \end{bmatrix} \tag{41}$$

Vector $\mathbf{d}^{(j)}$ is fed into the compensation routine c to provide updated $D^{(j)}(z)$. Figure 6 shows the autopilot summary.

Conclusion

A scheme for a digital adaptive autopilot has been described which uses identification and optimal synthesis process to compensate for time-varying dynamics of the aerospace vehicle. There are still some questions to be investigated. Notable among them are the proper choice of

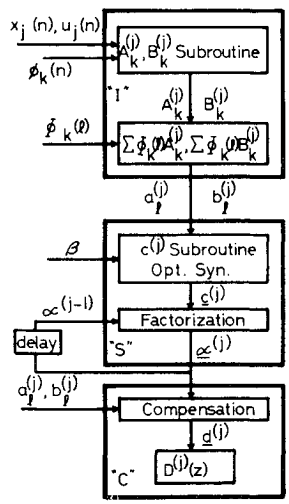

Fig. 6 Autopilot summary.

$\varphi_k(n)$ for identification and proper choice of performance index. Some experimentation with digital simulation is necessary to evaluate its effectiveness and to provide a basis for selecting the sampling time $T/2N$ and identification time T.

Appendix A: Airframe Differential Equations

Assuming linear aerodynamics, the equations of motion can be developed based upon the two-degrees-of-freedom longitudinal airframe differential equations, called the short-period approximation:

$$I\ddot{\theta} = M_{\alpha}\dot{\alpha} + M_{\delta c}\delta c, \qquad mV\dot{\gamma} = N_{\alpha}\alpha$$
$$\alpha = \theta - \gamma, \qquad a_N = (N_{\alpha}/M)\alpha \tag{A1}$$

where $M_{\dot{\alpha}} = C_{n\dot{\alpha}}SAMq$, $M_{\delta c} = C_{M\delta}qAL$, and $N_{\alpha} = C_{N\alpha}qA$. The variables θ, α, δ_c, and a_N represent the aircraft pitch rate, angle of attack, flap position, and normal acceleration. The coefficients M_{α} represent dimensional stability derivatives which need identification, and the quantities I, M, L, A, S, V, and q represent moment of inertia, mass, length, surface area, velocity, and dynamic pressure. If these equations are combined together, sampled and transformed, one obtains

$$G(z) = a_N(z)/\delta_c(z) = (a_1z^{-1} + a_2z^{-2})/(1 + b_1z^{-1} + b_2z^{-2}) \tag{A2}$$

Appendix B: Identification

Method 1: Based upon Correlation Functions

Assuming that various time functions in the closed-loop control systems are stationary, the input autocorrelation function is related to the output cross-correlation function as follows (see Fig. 1):

$$R_{ux}(n) = \sum_{m=0}^{\infty} k(m)R_{uu}(n - m) \tag{B1}$$

where

$$R_{ux}(n) = \lim_{N\to\infty} \frac{1}{2N+1} \sum_{j=-N}^{N} u(j)x(n + j) \tag{B2}$$

$$R_{uu}(n) = \lim_{N\to\infty} \frac{1}{2N+1} \sum_{j=-N}^{N} u(j)u(n + j) \tag{B3}$$

$k(m)$ = impulse response of system at $t = T_sm$. T_s = sampling period. Equation (B1) is of infinite order. But for stable system $k(m)$ tends to zero as m tends to infinity, it seems appropriate to replace the upper limit ∞ by a finite index l. Thus (B1) can be approximated truncated at $m = l$. Letting n vary from 0 to l yields a matrix equation

$$\mathbf{r}_{ux} = \mathbf{R}_{uu}\mathbf{k} \tag{B4}$$

where

$$\mathbf{r}_{ux} = \begin{bmatrix} R_{ux}(0) \\ R_{ux}(1) \\ \cdot \\ \cdot \\ \cdot \\ R_{ux}(l) \end{bmatrix}, \quad \mathbf{k} = \begin{bmatrix} k(0) \\ k(1) \\ \cdot \\ \cdot \\ k(l) \end{bmatrix} \tag{B5}$$

$$\mathbf{R}_{uu} = \begin{bmatrix} R_{uu}(0) & R_{uu}(1) \ldots & R_{uu}(l) \\ R_{uu}(1) & R_{uu}(0) \ldots & R_{uu}(l-1) \\ \cdot & & \\ \cdot & & \\ \cdot & & \\ R_{uu}(l) & R_{uu}(l-1) \ldots & R_{uu}(0) \end{bmatrix} \tag{B6}$$

Equation (B5) is solved to obtain the impulse response.

Method 2: Based upon Least-Square Approximation

If Equation (12) in the body of the paper is written in terms of input and output samples, one obtains

$$x_k = \sum_{l=0}^{m} a_l u_{k-l} - \sum_{l=1}^{m} b_l x_{k-l} \quad (b_0 = 1) \tag{B7}$$
$$k = 0, 1, \ldots, N$$

Equation (B8) can be rewritten as

$$x_k = \sum_{l=0}^{m} a_l^* u_{k-l} - \sum_{l=1}^{n} b_l^* x_{k-l} + e_k \tag{B8}$$

where a_l^*, b_l^* represent the predicted values and e_k the error. The quantities a_l^*, b_l^* are computed so that

$$\sum_{k=0}^{N} e_k^2 = \text{Minimum} \tag{B9}$$

This yields the solution of the form

$$\mathbf{a} = (\mathbf{A}^T\mathbf{A})\dagger\mathbf{A}^T\mathbf{x} \tag{B10}$$

where

$$\mathbf{a} = \begin{bmatrix} a_0 \\ \cdot \\ \cdot \\ \cdot \\ a_l \\ \\ b_1 \\ \cdot \\ \cdot \\ \cdot \\ b_l \end{bmatrix}, \quad \mathbf{x} = \begin{bmatrix} x_0 \\ x_1 \\ \cdot \\ \cdot \\ \cdot \\ x_n \end{bmatrix} \tag{B11}$$

T stands for transpose and $\dagger$ stands for pseudo inverse. Matrix $\mathbf{A}$ is in general rectangular, whose elements are u_k and x_k.

It should be remarked that for adaptive identification, instant by instant inversion of large matrices is very unsuitable for airborne computers.

References

[1] Andeen, R. E. and Shipley, J., "Digital Adaptive Flight Control System for Aerospace Vehicles," *AIAA Journal*, Vol. 1, No. 5, May 1963, pp. 1105–1109.

[2] Andeen, R. E., "Self Adaptive Autopilots," *Space/Aeronautics*, Vol. 43, No. 4, April 1965, pp. 46–52.

[3] Slaughter, J. B., "Compensating for Dynamics in Digital Control," *Control Engineering*, May 1964, U.S. Navy Electronics Laboratory, pp. 109–114.

[4] Kershow, "A Promising Experiment in Adaptive Control by Plant Identification," *Control Engineering*, Dec. 1965, U.S. Navy Electronics Laboratory, pp. 103–110.

[5] Puri, N. N., "Pulse Transfer Function Identification of a Linear System by Orthogonal Networks," 65WA/AUT, Nov. 16, 1965, American Society of Mechanical Engineers.

[6] Goodman, T. P. and Reswick, J. B., "Determination of System Characteristics from Normal Operating Records," *American Society of Mechanical Engineers Transactions*, Vol. 78, No. 2, 1956, pp. 259–271.

[7] Schaefekoetter, R. L. and Transier, K. G., "Parameter Identification: The Key to Second Generation Adaptive Flight Control," *Sperry Rand Engineering Review*, Vol. 17, pp. 25–32.

[8] Banon, R. L. et al, "Self-Organizing Adaptive Control of Aerospace Vehicles," *Proceedings of the 17th Annual National Electronics Conference* [NAECON], May 1965, p. 468.

[9] Kalman, R. E. and Englar, T., "Fundamental Study of Adaptive Control Systems," ASD-TR-61-27, Vol. 1 and Vol. 2, March 1961 and 1962, U.S. Air Force Aeronautical Systems Division.

[10] Letov, A. M., "Analytical Controller Design III," *Automation and Remote Control*, Vol. 21, No. 6, June 1960.

[11] Kalman, R. E., "Design of a Self-Optimizing Control System," *American Society of Mechanical Engineers Transactions*, Feb. 1958, pp. 468–478.